Artificial Intelligence-Based Deformation Analysis for Damage Identification in Structural Health Monitoring

Johanna STÄHLE[1,*], **Anastasiia VOLOVIKOVA**[2], **Steffen FREITAG**[3] and **Alexander STARK**[4]

These authors contributed equally to this work.

[1] *Institute of Concrete Structures and Building Materials (IMB), Concrete Structures Section, Karlsruhe Institute of Technology (KIT), Karlsruhe, Germany, (johanna.staehle@kit.edu)*

[2] *Institute of Structural Analysis (IBS), Karlsruhe Institute of Technology (KIT), Karlsruhe, Germany, (anastasiia.volovikova@kit.edu)*

[3] *Institute of Structural Analysis (IBS), Karlsruhe Institute of Technology (KIT), Karlsruhe, Germany, (steffen.freitag@kit.edu)*

[4] *Institute of Concrete Structures and Building Materials (IMB), Concrete Structures Section, Karlsruhe Institute of Technology (KIT), Karlsruhe, Germany, (alexander.stark@kit.edu)*

[*] *corresponding author*

Abstract

This paper investigates damage quantification through artificial neural networks. A feedforward neural network (FNN) and a convolutional neural network (CNN) is trained based on synthetic vibration displacements of a reinforced single-span concrete beam. The damage extent is modeled by crack patterns, which differ in crack lengths and number of cracks. Different levels of accuracy in the damage quantification are analyzed by investigating various classes of damage extents. The inputs of the CNN are vibration displacements whereas damage indicators are used for the FNN. High classification accuracies are obtained for both networks, which shows the benefit of artificial intelligence-based Structural Health Monitoring (SHM).

Keywords: Structural Health Monitoring, damage quantification, damage indicator, artificial neural network

1. Introduction

The continuous monitoring of structural integrity is essential, as undetectable damage can occur at any time during a structure's lifespan. Several Structural Health Monitoring (SHM) technologies have been developed so far to monitor the condition of a structure based on measurements. Using data-driven analysis methods, such as machine learning, information about the condition of structures can be extracted from a large amount of complex measured data (e.g. (Qi-Ang Wang et al., 2022; Tran-Ngoc et al., 2019; Memmolo et al., 2023; Volovikova et al., 2024)).

In this work, a method for determining damage extent using a feedforward neural network (FNN) and a convolutional neural network (CNN) to process vibration displacement data is presented. First, a concrete beam with variable damage extent (different crack patterns) is modeled. This allows a clear specification of the characteristics of the damaged structure. The finite element (FE) model is then used to generate a synthetic dataset. Subsequently, a CNN is trained to predict the extent of damage based on the vibration displacement time histories. In another approach, the dimension of time histories is reduced by expressing them as damage indicators. Four common damage indicators are investigated and used to train a FNN to classify the damage extent.

2. Numerical beam experiment

The numerical beam model was established to a previous own test on a reinforced concrete beam

(Kohm, 2021). In the experiment, the beam was loaded by different load steps, which created bending cracks. The test was carried out displacement-controlled to achieve predefined beam deflections. After achieving each load step, the crack pattern was documented and afterwards the load was removed and the beam was excited by an impulse through a rubber hammer. The structural response was measured with MEMS (micro-electromechanical system) acceleration sensors with a sampling frequency of 4000 Hz. Since the vibration measurement data of those experiments are not sufficient for machine learning, synthetic vibration data are generated by a linear elastic numerical beam model.

2.1 Finite element model

The beam is modeled with software environment Abaqus. The single-span beam has a length of 6.5 m and a cross section of 0.2 m x 0.3 m. The concrete with a Young's Modulus of 31,580 MPa and a density of 2294 kg/m^3 is modeled through C3D20 elements to map the dynamic behavior of the structure. The element size is determined to 25 mm x 50 mm x 50 mm. The longitudinal reinforcement (f_{yk} = 500 MPa) has a diameter of 14 mm, whereas the stirrups have a diameter of 8 mm with spacing of 200 mm. Near the supports the distance of stirrups was reduced to 80 mm to prevent a shear failure. The Young's Modulus for reinforcement is 200,000 MPa. The reinforcement is modeled through T3D2 elements. The modeled experiment was a 3-point-bending test.

In a frequency step, the eigenvalue extraction using the automatic multi-level substructuring (AMS) eigensolver is selected. The faster eigenvalue extraction method AMS is chosen rather than Lanczos method. The vibration data are generated through a modal dynamic step. For linear dynamic analysis based on modal superposition, several options are provided in Abaqus to introduce damping. In this work, damping is considered by a critical damping factor. The equation of motion for a one degree of freedom system is

$$m\ddot{q} + c\dot{q} + kq = 0, \tag{1}$$

where m is the mass, c the damping, k the stiffness, and q the modal amplitude. The solution is of the form

$$q = A^{\lambda t}, \tag{2}$$

where A is a constant, and

$$\lambda = \frac{-c}{2m} \pm \sqrt{\frac{c^2}{4m^2} - \frac{k}{m}}. \tag{3}$$

Critical damping is defined as

$$c_{cr} = 2\sqrt{mk}\,. \tag{4}$$

The fraction of critical damping is

$$\xi = \frac{c}{c_{cr}}, \tag{5}$$

where c is the damping of that mode shape and c_{cr} is the critical damping. The fraction of critical damping ξ associated with each mode can be defined by direct modal damping. Typically, values in the range of 1% to 10% of critical damping are used. In this work, the critical damping fraction is set to $\xi = 0.05$ for all considered modes.

2.2 Model verification and validation

The dynamic structural simulation should map the dynamic behavior of the real beam. The verification and validation of the finite element model is conducted in two steps. First, through a comparison of the natural frequencies of the undamaged (uncracked) beam with the analytical solution (model verification). Second, through a comparison of the change of the natural frequency in dependence of the load step (cracking state) of the numerical and the real measured first natural frequency (model validation).

2.2.1 Verification of the finite element model using the analytical solution of the natural frequencies

First, an unreinforced concrete beam, supported at mid-depth, is modeled. The boundary conditions at the left support are $u_x = u_y = u_z = 0$ and at the right support $u_y = u_z = 0$. The finite element model is verified using the analytical solutions of the natural frequencies of a single-span beam. The natural frequencies of a simply supported beam can be expressed as

$$f_n = \frac{n^2\pi}{2L^2}\sqrt{\frac{EI}{\overline{m}}} \quad for \quad n = 1, 2, 3, \dots, \tag{6}$$

where EI is the bending stiffness, $\overline{m}$ is the length-related mass, L is the beam length and n is the mode number. The first three analytical and numerical natural frequencies of the undamaged concrete beam are shown in Table 1. It can be seen, that the FE results are close to the analytical solution.

Table 1. Analytical and numerical natural frequencies of a simply supported concrete beam

Frequency	Analytical	FE model
f_1	11.94 Hz	11.90 Hz
f_2	47.79 Hz	47.13 Hz
f_3	107.52 Hz	104.39 Hz

Figure 1 shows the first three bending mode shapes of the unreinforced, mid-depth supported, FE model.

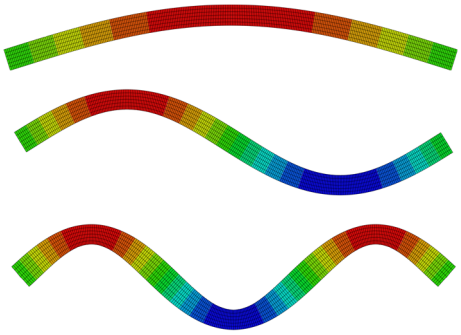

Figure 1. First three bending mode shapes of the FE model

Adding the reinforcement with embedded elements and arranging the boundary conditions similar to the real experimental setup on the downside of the beam, each 50 mm from the end of the beam, results in slightly different natural frequencies, see Table 2.

Table 2. Natural frequencies of the reinforced concrete beam FE model

Frequency	Final model
f_1	12.66 Hz
f_2	49.03 Hz
f_3	98.50 Hz

2.2.2 Validation of the finite element model using the experimental results

In order to simulate damage, the crack pattern observed during the real experimental test according to different load steps is inserted into the FE model. It should be noted, that only crack widths ≥ 0.1 mm are considered. Figures 3(a) and 3(b) show a comparison between the real and the numerically modeled crack pattern of load step LS16. The crack patterns of every load level differ in crack length and number of cracks. The model calibration and validation is carried out by reducing the Young's Moduli of the cracked elements in such a way that the natural frequency change of the real experiment is achieved. Figure 2 shows the evolution of the natural frequencies (in percentage of the undamaged beam) depending on the load step for the experiment and the FE model. Significant cracks initially occurred at load step LS05.

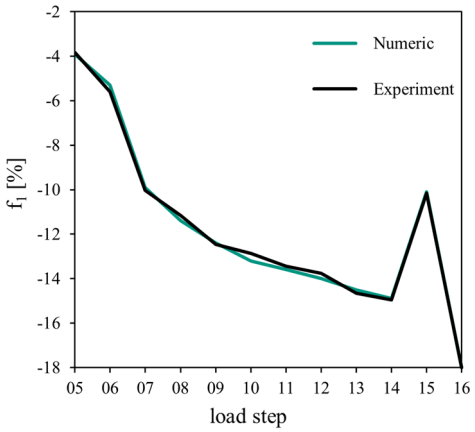

Figure 2. Evolution of the first natural frequency with respect to increasing damage (load steps) – results of the experiment and the calibrated FE model (numeric)

2.3 Generation of synthetic vibration deformation data

The vibration of the beam is generated with a modal dynamic step. The weight of the beam itself was not taken into account in this step for the sake of simplicity. Impulse excitations are induced by a rubber hammer through concentrated impulse forces of 10 N. The impulses are introduced at five different positions (Pos. 1 - Pos. 5) shown in Figure 3(c). In Table 3, the positions of the investigated impulse excitation with regard to the left beam end are presented. The impulse forces are introduced at the mode shape maxima of the first to the third mode shapes and the superposition of these mode shapes. The vibration displacement is monitored at 25 virtual sensors with a distance of 25 cm each at the upside of the beam as shown in Figure 3(c).

Table 3. Position of the excitation points

Position	1	2	3	4	5
x in mm	3375	4550	4900	5125	5400

At each excitation position, two impulse signals are modeled as triangular impulses with a length of 0.003 or 0.002 s, respectively. The lead time until the start of the impulse is chosen to 0.1 s. The total signal length is 1 s.

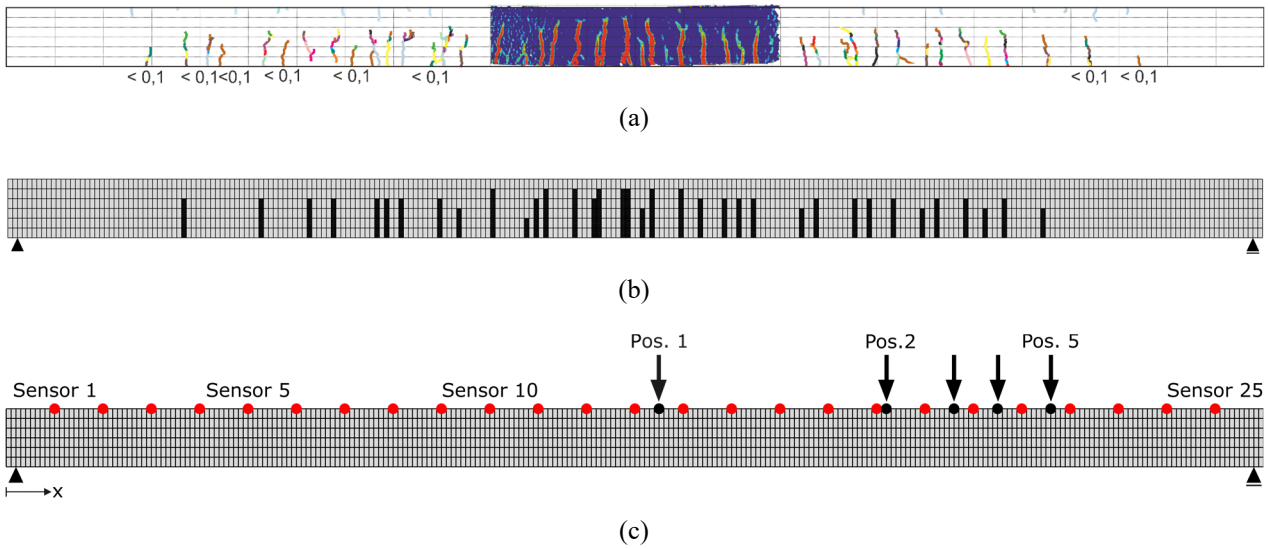

Figure 3. Comparison of experimental (a) and modeled (b) crack pattern of load step LS16; (c) sensor positions (1 - 25) and positions of impulse excitation (Pos. 1 - Pos. 5)

3. Artificial intelligence-based models

Two distinct classification network models are developed to predict the degree of damage of the beam using vibration displacement simulation data. The first model is an artificial neural network with feedforward architecture (FNN), while the second model is a convolutional neural network (CNN). The following sections describe both artificial neural network models, including dataset preparation, input formats, network architectures, and training parameters.

3.1 Dataset preparation

Both models utilize synthetic vibration displacement data of the beam. The CNN processes the data as time series of vibration displacements, whereas for the FNN, damage indicators (DIs) are calculated from the displacement data to reduce the dimensionality of the input. For both networks, 130 samples are available, derived from 13 load steps (LS), with 2 impulses at 5 different excitation positions.

The output of both classifier networks indicates the corresponding damage state of the beam. Three classification scenarios are elaborated, including two, three, and four classes of damage states defined by the maximum crack width as damage extent, see Table 4, in order to compare the performance accuracy of the networks across multiple classes.

Table 4. Classification scenarios defined by the maximum crack width as the damage extent at different load steps

Load Steps	Crack width		
	2 Classes	**3 Classes**	**4 Classes**
LS00	< 0.2 mm	< 0.2 mm	-
LS05			< 0.2 mm
LS06			
LS07			
LS08			
LS09	≥ 0.2 mm	≥ 0.2 mm < 0.3 mm	≥ 0.2 mm < 0.3 mm
LS10			
LS11			
LS12			
LS13		≥ 0.3 mm	≥ 0.3 mm
LS14			
LS15			
LS16			

While the CNN can process the time series of vibration displacements from each of the 25 sensors directly, the time series data for the FNN must be converted to reduce the input dimension. Consequently, damage indicators (DIs) are calculated from the data signals acquired in the FE model. In this work, four damage indicators (DIs) are computed from the time series of the vibration displacements. The DIs are calculated using the vibration displacement time history acquired

through 25 sensors at the pristine state (load step LS00) $x_B(k)$ and the current (undamaged or damaged) state $x_C(k)$ (load step LS00 – LS16) of the structure at time step k. In the following equations, N represents the maximum number of data points, which is equal to 4001 time steps in this work. The first DI is based on the differential vibration displacement

$$DI_E = \sum_{k=1}^{N}(x_C(k) - x_B(k))^2, \quad (7)$$

the second DI relies on the root-mean-square deviation of the vibration displacements

$$DI_{RMSD} = \sqrt{\frac{\sum_{k=1}^{N}(x_C(k)-x_B(k))^2}{\sum_{k=1}^{N} x_B(k)^2}}, \quad (8)$$

the third DI employs the Pearson correlation coefficient of the vibration displacements

$$DI_{CC} = 1 - \frac{\sum_{i=1}^{n}(x_C(k)-\bar{x}_C)(x_B(k)-\bar{x}_B)}{\sqrt{\sum_{i=1}^{n}(x_C(k)-\bar{x}_C)^2}\sqrt{\sum_{i=1}^{n}(x_B(k)-\bar{x}_B)^2}}, \quad (9)$$

and the fourth DI is determined by the generalized difference between the vibration displacements

$$DI_{GE} = \frac{\sum_{k=1}^{N}(x_C(k-1)+x_C(k))^2 - \sum_{k=1}^{N}(x_B(k-1)+x_B(k))^2}{\sum_{k=1}^{N}(x_B(k-1)+x_B(k))^2}. \quad (10)$$

As an example, DI_{CC}, calculated for Impulse 2 at Position 3 for each load step, is presented in Figure 4. Each line represents one of the 25 sensors, where the displacement is measured. As the load steps evolves, the difference in vibration displacement compared to the pristine state (LS00) increases, resulting in an ascending trend for the DI except for LS15.

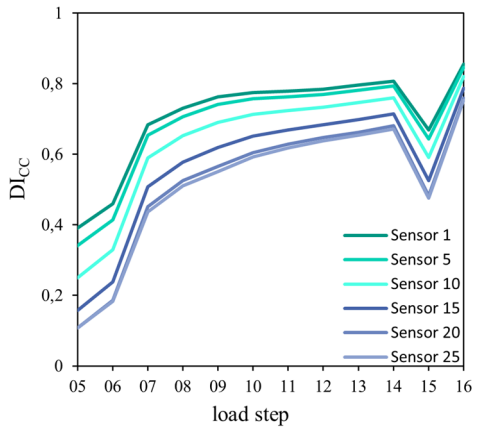

Figure 4. Damage indicator DI_{CC} calculated for Impulse 2 at Position 3 for each load step

These calculated DIs are used as inputs for the FNN. Each type of DI is investigated in separate FNN models. An example of one input sample of a FNN is shown in Figure 5.

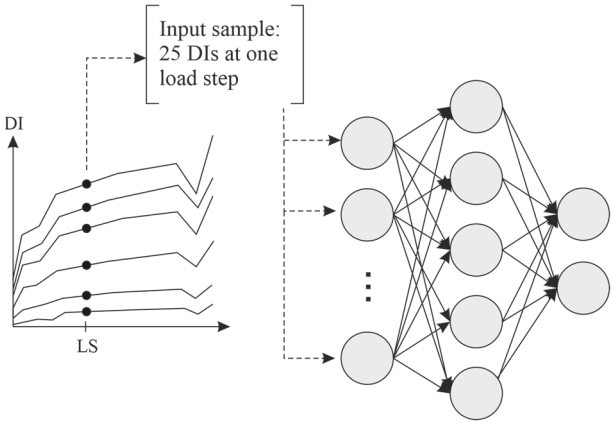

Figure 5. DIs used as inputs for the FNN model

3.2 Feedforward neural network

The FNN used in this work is a fully connected network, which consists of 25 input neurons, each corresponding to a damage indicator from one of the 25 sensors, two hidden layers with 5 neurons each, and one output layer with as many neurons as there are classes, corresponding to the class definitions in Table 4. The hidden neurons are activated by the hyperbolic tangent sigmoid transfer function (tansig) and the softmax transfer function is used in the output neurons for multiclass classification.

The Levenberg-Marquardt-Algorithm is selected to train the FNN, with 70% of the 130 samples allocated for identifying the unknown network parameters (synaptic weights and bias values), 15% for validation, and 15% for testing. To avoid overfitting, the network parameter set, which results in the lowest validation error, is finally selected.

3.3 Convolutional neural network

The basic idea of the second approach is similar to the previous one, where information obtained from the measured vibration displacements serves as input. However, instead of using DIs, the vibration displacements are retained in their time series form to leverage the strengths of a CNN. The architecture of the CNN is presented in Table 5.

The CNN is trained using the Adam optimizer with an initial learning rate of 0.001. Cross-entropy is used as a loss function for classification task. The training process is conducted over 200 epochs with a mini-batch size of 16. The data is shuffled at the

beginning of each epoch to ensure randomness and prevent overfitting. Similar to the FNN training, 70% of the data is used for training and 15% each for validation and testing.

Table 5. CNN architecture

Layer	Parameters
Sequence Input	[25, 4001]
Convolution 1D	Filters: 16, Size: 5, Stride: 1, Padding: same
Batch Normalization	-
ReLU	-
Max Pooling 1D	Pool Size: 2, Stride: 2
Convolution 1D	Filters: 32, Size: 5, Stride: 1, Padding: same
Batch Normalization	-
ReLU	-
Global Average Pooling 1D	-
Flatten	-
Fully Connected	Neurons: 32
ReLU	-
Dropout	Dropout Rate: 0.5
Fully Connected	Neurons: number of classes
Softmax	-
Output	Neurons: 2-4

As already mentioned for the FNN, the output layer of the CNN also consists of as many neurons as classes to be predicted.

It should be noted that for both, the FNN and the CNN, the number of hidden layers, neurons, and training options are optimized through trial and error. While other architectures and training parameters could potentially yield better results, exploring these alternatives is beyond the scope of this paper.

4. Results and discussion

The results of both AI models are presented in Figures 6 and 7, as well as in Table 6. The output of each model is displayed in the form of confusion matrices, which compare the predicted classes with the true classes. These confusion matrices are divided into matrices for training, validation, and test data, as well as for all data combined. Each confusion matrix shows the prediction accuracy of the model, which is evaluated by comparing how often the model correctly predicted the true class and how often it made false predictions. In Figures 6 and 7, the results for both AI models are exemplarily presented for one network model for the 4-class classification problem. For the FNN model, the variant with DI_{CC} as input is selected, as this input type achieved the best results for the network, as can be seen in Table 6.

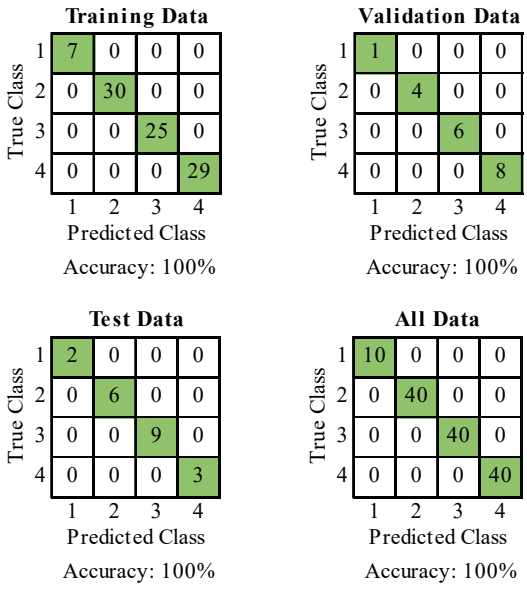

Figure 6. FNN performance accuracy for 4-class classification by DI_{CC}-Input

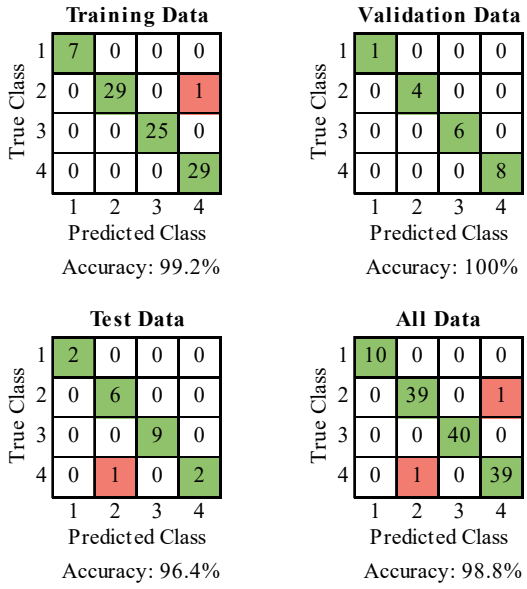

Figure 7. CNN performance accuracy for 4-class classification

Table 6 summarizes the results in terms of prediction accuracy on the test data for both AI models. Each accuracy percentage represents an average value, calculated over ten independently produced network models, providing a better representation of the prediction performance.

Additionally, Table 6 distinguishes between models with four different damage indicator inputs for the FNN. The columns also allow a comparison of the model performances across different classification scenarios (2-class, 3-class, and 4-class classification). The performance accuracy evaluation primarily focuses on the test data, which were not used within training.

Table 6. AI-models prediction accuracy for the test data

AI-models		2-class	3-class	4-class
FNN	DI_E	93.5%	74.5%	72.5%
	DI_{RMSD}	93.3%	88.5%	86.0%
	DI_{CC}	96.0%	96.5%	98.5%
	DI_{GE}	81.0%	55.0%	65.5%
CNN		92.5%	91.0%	92.5%

The results clearly show that both AI-models effectively can handle the classification task with varying numbers of classes.

Due to the compressed DI input, a smaller network with fewer parameters (FNN) can be successfully trained. Whereas for the entire vibration displacement time histories a larger network (CNN) is required.

The FNN demonstrates better performance compared to the CNN if the DI_{CC} is used as input and worse performance for the remaining DIs. A decreasing trend is awaited with an increasing number of classes. The more classes to be predicted, the less data is available for training each class, which consequently is expected to reduce the model's performance. This trend is only partially observed, as all models (except the FNN with DI_{CC}) perform better in the 2-class scenario than in the 3- or 4-class scenarios. The difference between the 3- and 4-class scenarios is not clearly discernible.

It is important to note that no generalization has yet been made to any vibration displacement data from unknown impulse or excitation positions.

5. Conclusions

This paper investigates damage quantification using artificial intelligence (AI)-based models, specifically focusing on synthetic vibration displacements of a reinforced single-span concrete beam. Initially, an FE model of the concrete beam with variable damage extents was built, allowing for a clear specification of the damaged structure's characteristics. The damage extent was represented by varying crack patterns in terms of crack lengths and the number of cracks. This model was then used to generate a synthetic dataset of vibration deformations.

Two AI-based models, an artificial neural network with a feedforward architecture (FNN) and a convolutional neural network (CNN), were generated to classify the state of the beam structure. A CNN was employed to predict the extent of damage based on vibration displacement time histories. Additionally, the time histories were reduced to damage indicators, which were used to train a FNN for the same classification task.

Different levels of accuracy in damage quantification were analyzed by examining various classes of damage extents. Each artificial neural network was designed and tested in 2-class, 3-class, and 4-class classification scenarios, determined relative to the damage extent (maximum crack width). For each model, the predictions about the structure's condition were compared using confusion matrices to evaluate the performance accuracy. The results demonstrate that both, FNN and CNN approaches, can classify the state of the simulated beam model regarding the damage extent using vibration displacement data or damage indicators derived from it. Notably, both CNN and FNN with DI_{CC} achieve high accuracy in the presented examples.

Future work should focus on refining the beam model, incorporating noise in the vibration displacement data, and optimizing neural network architectures to further improve the performance. Additionally, removing an excitation position from the training set for generalization testing, exploring more classes, and using both measured and simulation data with added noise will further establish the background for future monitoring tasks.

References

Kohm, M. (2021). *Entwicklung eines Messsystems zur modalbasierten Schädigungsanalyse von Brückenüberbauten.* Dissertation. https://doi.org /10.5445/KSP/1000145597

Memmolo, V.; Moll, J.; Schackmann, O.; Freitag, S.; Volovikova, V.; Tschöke, K.; Savli, E.; Lugovstova, Y.; Moix-Bonet, M.; Bayoumi, A.; Mueller, I. (2023). *Promoting Novel Strategies for the Reliability Assessment of Guided Wave Based*

SHM Systems. Proceedings of the 14th International Workshop on Structural Health Monitoring (IWSHM), DEStech Publications, Inc.

Qi-Ang Wang, Yang Dai, Zhan-Guo Ma, Yi-Qing Ni, Jia-Qi Tang, Xiao-Qi Xu, & Zi-Yan Wu. (2022). *Towards probabilistic data-driven damage detection in SHM using sparse Bayesian learning scheme.* Structural Control and Health Monitoring. https://doi.org/10.1002/stc.3070

Tran-Ngoc, H., Khatir, S., Roeck, G., Bui-Tien, T., & Abdel Wahab, M. (2019). *An efficient artificial neural network for damage detection in bridges and beam-like structures by improving training parameters using cuckoo search algorithm.* Engineering Structures, Vol. 199, https://doi.org/10.1016/j.engstruct.2019.109637.

Volovikova, A., Freitag, S., Schackmann, O., Memmolo, V., Bayoumi, A., Mueller, I., & Moll, J. (2024). *Artificial Intelligence-Based Approach for Damage Localization in Ultrasonic Guided Wave-Based Structural Health Monitoring.* Structural Health Monitoring in the Light of Climate Impact and Data Science. Research and Review Journal of Nondestructive Testing Vol. 2(2).